Annals of Nuclear Cardiology Vol. 5 No. 1 141–159

This article is being jointly published in the Annals of Nuclear Cardiology and the Journal of Nuclear Cardiology.

SPECIAL REVIEW ARTICLE: JSNC RECOMMENDATION (JNC JOINT PUBLICATION)

Recommendations for ^{18}F-Fluorodeoxyglucose Positron Emission Tomography Imaging for Diagnosis of Cardiac Sarcoidosis－2018 Update: Japanese Society of Nuclear Cardiology Recommendations

Shinichiro Kumita, MD, PhD[1], Keiichiro Yoshinaga, MD, PhD, FACC, FASNC[2], Masao Miyagawa, MD, PhD[3], Mitsuru Momose, MD, PhD[4], Keisuke Kiso, MD, PhD[5], Tokuo Kasai, MD, PhD[6] and Masanao Naya, MD, PhD[7]
Committee for diagnosis of cardiac sarcoidosis using ^{18}F-FDG PET, Japanese Society of Nuclear Cardiology

Received: December 19, 2018/Revised manuscript received: January 9, 2019/Accepted: January 12, 2019
J-STAGE advance published: June 18, 2019

This manuscript was previously published in Shinzo-Kaku-Igaku in Japanese [Kumita S, Yoshinaga K, Miyagawa M et al. 心臓サルコイドーシスに対する^{18}F-FDG PET検査の手引き 2018年改訂. Shinzo-Kaku-Igaku 21: 22-27_14 https://doi.org/10.14951/jsnc.21-001]. This manuscript is an English translated version with some modifications.

Sarcoidosis is a systemic inflammatory disorder of unknown etiology affecting people of any age (1, 2). The disease shows heterogeneous distribution of epithelioid granulomatous inflammation without caseous necrosis and unpredictable clinical course (3). Divergent phenotypes have been identified, and sarcoidosis lesions may involve multiple organs, including the lungs, lymph nodes, eyes, bones, liver, spleen, skin, muscles, nervous system and heart. Although about 20% of patients have chronic progression, in general the inflammation spontaneously resolves, and, therefore, sarcoidosis was previously believed to be a benign disease. However, cardiac involvement is associated with a poor prognosis, accounting for 13% to 25% of deaths from sarcoidosis (4). The most common causes of death are fatal ventricular arrhythmias and heart failure (1). Therefore, early detection and treatment are crucial.

Guidelines for the diagnosis of cardiac sarcoidosis (CS) were first published in 1992 (5) and then revised in 2006 in Japan (6). Cardiac involvement had been considered an infrequent manifestation; however, an autopsy investigation revealed a substantially higher occurrence, up to 50% in Japan (7). Revisions to the guidelines have been made with the aim of improving CS diagnosis by including consideration of histopathological criteria and frequently recognized and characteristic clinical manifestations such as advanced atrioventricular block and thinning of basal interventricular septum. Following revision of the Japanese guidelines, the significance of CS has been reconsidered, and many patients with previously undiagnosed CS have been identified. However, diagnosis of CS is still challenging because the histological detection rate of CS is very low, and CS is difficult to distinguish from some other diseases, such as dilated cardiomyopathy. Recently, there have been substantial developments in several cardiac imaging modalities including cardiac magnetic resonance imaging (MRI), ^{18}F-fluorodeoxyglucose (^{18}F-FDG) positron emission tomography

doi: 10.17996/anc.19-00092

1) Department of Radiology, Nihon Medical University, Japan
2) Diagnostic and Therapeutic Nuclear Medicine, National Institutes for Quantum and Radiological Science and Technology, National Institute of Radiological Sciences, Japan
3) Department of Radiology, Ehime University Graduate School of Medicine, Japan
4) Department of Diagnostic Imaging and Nuclear Medicine, Tokyo Women's Medical University, Japan
5) Department of Radiology, National Cerebral and Cardiovascular Center, Japan
6) Department of Cardiology, Niigata University School of Medicine, Japan
7) Department of Cardiology, Hokkaido University Graduate School of Medicine, Japan

Table 1 2017 JCS Diagnostic guidelines for cardiac sarcoidosis (12)

Histological diagnosis group (those with positive myocardial tissue findings)	Cardiac sarcoidosis diagnosed histologically when endomyocardial biopsy or surgical specimens demonstrated non-caseating epithelioid granuloma
Clinical diagnosis group (those with negative myocardial tissue findings or those not undergoing myocardial biopsy)	The patient is clinically diagnosed as having sarcoidosis (a) when epithelioid granulomas are found in organs other than the heart, and clinical findings strongly suggestive of the below-mentioned cardiac involvement are present; or (b) when the patient shows clinical findings strongly suggestive of pulmonary or ophthalmic sarcoidosis or at least two of the five characteristic laboratory findings of sarcoidosis (Table 4); and clinical findings strongly suggestive of the below-mentioned cardiac involvement are present.
Major criteria	1. High-grade atrioventricular block (including complete atrioventricular block) or fatal ventricular arrhythmia (e.g., sustained ventricular tachycardia and ventricular fibrillation) 2. Basal thinning of the ventricular septum or abnormal ventricular wall anatomy (ventricular aneurysm, thinning of the middle or upper ventricular septum, regional ventricular wall thickening) 3. Left ventricular contractile dysfunction (left ventricular ejection fraction of less than 50%) 4. ^{67}Ga-citrate scintigraphy or ^{18}F-FDG PET reveals abnormally high tracer accumulation in the heart 5. Gadolinium-enhanced MRI reveals delayed contrast enhancement of the myocardium
Minor criteria	1. Abnormal ECG findings: Ventricular arrhythmias (nonsustained ventricular tachycardia, multifocal or frequent premature ventricular contractions), bundle branch block, axis deviation, or abnormal Q waves 2. Perfusion defects on myocardial perfusion scintigraphy (SPECT) 3. Endomyocardial biopsy: monocyte infiltration and moderate or severe myocardial interstitial fibrosis
Cardiac involvement	Cardiac findings should be assessed based on the major criteria and the minor criteria. Clinical findings that satisfy the following 1) or 2) strongly suggest the presence of cardiac involvement. 1. Two or more of the five major criteria (a) to (e) are satisfied. 2. One of the five major criteria (a) to (e) and two or more of the three minor criteria (f) to (h) are satisfied.

^{18}F-FDG: fluorodeoxyglucose

(PET), and echocardiography. Of these, cardiac MRI with late-gadolinium enhancement (LGE) can detect fibrosis, which is usually located in the mid and/or epicardial layer rather than endocardial layer in CS (8). LGE can find about 80% of CS cases (9). ^{18}F-FDG PET detects active inflammation as a positive uptake in CS. The characteristic findings of echocardiography include basal interventricular septal wall thinning and regional myocardial abnormalities such as aneurysm. These advanced forms of cardiac imaging are better able to detect CS than is endomyocardial biopsy, the diagnostic sensitivity of which is only 20% (10), much lower than that of cardiac imaging. Inflammatory lesions of CS are usually located in the mid and/or epicardial layers of myocardium with patchy distribution as determined by MRI with LGE and autopsy studies. This may be one of the reasons for the low diagnostic accuracy of endomyocardial biopsy (11). The lower sensitivity of histopathology-based diagnosis than of image-based diagnosis makes it unsuitable for optimal disease management. This being the case, in February 2017, the Japanese Circulation Society (JCS) published new guidelines for diagnosis and treatment of CS (Table 1) (12). The new guidelines outline the diagnostic approach to CS. Diagnosis of CS is divided into 2 categories, histologically positive findings (histological diagnosis group) and negative or no histological findings (clinical diagnosis group). These updated guidelines contain additional diagnostic criteria for cardiac involvement in sarcoidosis: 1) Fatal ventricular arrhythmia and high-grade atrioventricular block were added to the major criteria; 2) Abnormal ventricular wall anatomy was upgraded from inclusion in the minor criteria to inclusion in the major criteria next to the basal septal wall thinning; 3) Abnormally high tracer accumulation in the heart as identified by ^{18}F-FDG PET was moved from the minor diagnostic criteria to the major diagnostic criteria, which already included abnormally high tracer accumulation as revealed by ^{67}Ga-citrate scintigraphy. This finding reflects active inflammation and may indicate the need for steroid therapy and treatment monitoring; 4) The LGE of the myocardium in gadolinium-enhanced MRI was upgraded from the minor diagnostic criteria to the major diagnostic criteria. LGE can identify myocardial fibrosis.

The updated JCS guidelines also introduced diagnostic criteria for isolated CS because isolated CS is more common than previously reported, representing 5%–15% of all sarcoidosis cases (13, 14).

Early detection of CS is essential in order to provide timely and appropriate treatment approaches that may result in better outcomes. For early detection of CS, imaging modalities such as cardiac MRI and ^{18}F-FDG PET play important roles. Myocardial perfusion single-photon emission computed tomography (SPECT) using ^{201}Thallium (^{201}Tl) and ^{99m}Techneti um-labeled radiopharmaceutical (^{99m}Tc) can also detect myocardial scarring as a perfusion defect, especially in the basal septum. However, both sensitivity and specificity of

those myocardial perfusion imaging (MPI) modalities are somewhat low for detecting CS. Therefore, cardiac MRI is upgraded to the major criteria. On the other hand, myocardial perfusion SPECT is included in the minor criteria. Although cardiac MRI has excellent spatial resolution and is free from radiation exposure, the gadolinium contrast agent may be harmful and should be avoided for patients with chronic kidney disease. In such cases, T2-weighted short Ti inversion recovery imaging is useful in assessing myocardial edema, and T1 mapping shows promise for estimating extra-cellular volume and scarring.

In order to develop a treatment strategy, it is important to determine whether there is inflammatory activity, to assess the severity, and to predict the outcome. For this purpose, ^{67}Ga-citrate scintigraphy has traditionally been used for detecting active inflammatory lesions (15). However, ^{67}Ga scintigraphy is less sensitive for detecting mild to moderately active CS lesions because of its low spatial resolution. Therefore, negative ^{67}Ga scintigraphy findings do not always indicate an inactive disease status. This being the case, ^{18}F-FDG PET has emerged as an alternative approach to ^{67}Ga scintigraphy for detecting CS.

^{18}F-FDG accumulates in cells with increased glucose metabolism such as cancer cells and inflammatory cells. “Pathological” glucose uptake is regulated mainly by glucose transporters (GLUT) 1 and 3. GLUT1 and GLUT3 accumulate on the cell membrane in patients with cancers and inflammatory diseases, such as vasculitis and sarcoidosis. On the other hand, physiological glucose uptake by myocardial cells is regulated mainly by GLUT4. As the blood glucose level and/or insulin level increases, the physiological glucose uptake increases via GLUT4. It is possible to distinguish between “pathological” and “physiological” ^{18}F-FDG uptake through the use of a long-fasting preparation before evaluation. Suppressing physiological myocardial ^{18}F-FDG uptake is the key to obtaining ^{18}F-FDG PET imaging to accurately assess inflammatory activity of CS. Quantification of ^{18}F-FDG uptake is generally expressed as a standardized uptake value (SUV). However, a cut-off value for diagnosis of active inflammation has not been established. Nonetheless, an SUV may be used to assess the inflammatory activity and to monitor the treatment efficacy. After successful treatment, sarcoidosis disease activity remains stable for a certain length of time but often recurs. ^{18}F-FDG PET can also detect the recurrence of sarcoidosis.

The Japanese Ministry of Health, Labour and Welfare (JMHLW) approved ^{18}F-FDG PET use for detecting cardiac sarcoid lesions and began reimbursement in March 2012 (16, 17). To date, Japan is the only country to provide governmental approval and reimbursement of ^{18}F-FDG PET for such a purpose. In 2013, the Japanese Society of Nuclear Cardiology (JSNC) issued the first set of recommendations for ^{18}F-FDG PET use in CS (18), four years before the American Society of Nuclear Cardiology (ASNC) published its expert consensus document on ^{18}F-FDG PET use in CS (19). Since publishing the initial version in 2013, we have found new evidence related to ^{18}F-FDG PET use for diagnosis of CS (20, 21). In addition, the updated 2017 JCS guidelines upgraded the role of ^{18}F-FDG PET for diagnosis of CS. Based on the recent development and the updated JCS guidelines, JSNC decided to update the recommendations regarding ^{18}F-FDG PET use in CS.

^{18}F-FDG PET guidelines in the diagnosis of cardiac sarcoidosis

[1] Patient preparation for ^{18}F-FDG PET: method for suppressing physiological myocardial ^{18}F-FDG uptake in normal myocardium

Over 90% of fasting myocardial energy metabolism is fatty acid metabolism. Most of the remaining 10% of metabolism involves other substances including glucose (22, 23). However, fasting myocardial glucose metabolism varies among individuals, and in some cases, myocardial ^{18}F-FDG uptake is observed even under fasting conditions. This discrepancy means it is difficult to use ^{18}F-FDG PET for myocardial inflammation imaging and diagnostic accuracy may be affected. Therefore, some groups have evaluated approaches to suppressing myocardial physiological glucose use (^{18}F-FDG uptake). Currently, the following three approaches are considered to be effective (24).

1. Pre-^{18}F-FDG PET fasting time

It is necessary to administer ^{18}F-FDG and perform ^{18}F-FDG PET image acquisition under fasting conditions (25). In order to accurately diagnose CS, it is essential to produce a condition of high ^{18}F-FDG uptake in a myocardial sarcoidosis lesion without physiological ^{18}F-FDG uptake in normal myocardium. Therefore, the ^{18}F-FDG protocol for diagnosis of CS is a fasting protocol (Figure 1). However, the optimum fasting time for diagnosis of CS has not yet been established. In its guidelines for oncology diagnosis, the European Association of Nuclear Medicine recommends fasting for at least 6 hours in order to suppress ^{18}F-FDG uptake in normal tissues (26).

Many ^{18}F-FDG PET studies for detecting CS, published since 2004, have used a fasting time of over 12 h (Table 2). A report that reviewed five previously published papers shows a diagnostic sensitivity of 91% and specificity of 75.5% in the diagnosis of CS using ^{18}F-FDG PET (25). A meta-analysis by Youssef et al. showed a diagnostic sensitivity of 89% and

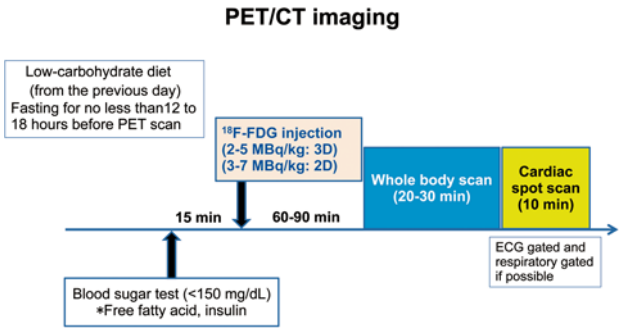

Figure 1 ^{18}F-FDG PET/CT scan protocol for diagnosis of cardiac sarcoidosis.
- Patient preparations include low-carbohydrate diet and prolonged fasting (no less than 12–18 h) are recommended.
- Blood tests should include blood sugar prior to ^{18}F-FDG administration.
- Dose of ^{18}F-FDG administered should be based on the recommendations in the guidelines of the JSNM (57).
- In the case of positive cardiac ^{18}F-FDG uptake with whole-body imaging, subsequent cardiac spot imaging is recommended.
- *Blood tests including free fatty acid and insulin levels are recommended if possible.

Reprinted with permission from (96).

specificity of 78% in the diagnosis of CS by ^{18}F-FDG PET (27). Most of the papers reviewed in the above two articles used fasting conditions of greater than 12 hours. Attention is paid to the high sensitivities, while the low specificity and high variability are also highlighted especially by the meta-analysis (27). The greatest cause of low specificity and high variability seems to be associated with physiological ^{18}F-FDG uptake in normal myocardium. Early PET studies, especially before 2004, used shorter fasting times, and these early reports enrolled patients with diffuse myocardial ^{18}F-FDG uptake under insufficient dietary preparation. Therefore, these early studies might have misdiagnosed CS, and insufficient dietary preparation might have accounted for the lower diagnostic specificity. Appropriate preparation for ^{18}F-FDG PET study is essential in order to accurately diagnose CS using ^{18}F-FDG PET.

Langah et al. examined the diagnostic utility of an 18-h fasting preparation (28), and they reported a diagnostic sensitivity of 85% and specificity of 90% in the diagnosis of CS using ^{18}F-FDG PET. They indicated that with 18 h of fasting preparation, there was an improvement in specificity, and that the ^{18}F-FDG myocardial-to-blood pool ratio decreased more significantly under the 18-h fasting condition than under a shorter fasting condition. However, recent studies using normal volunteers showed that there were more than a few cases with positive ^{18}F-FDG myocardial physiological uptake even under more than 18 h of fasting before PET study (29, 30). Manabe et al. reported that an 18-h fasting protocol combined with a carbohydrate-restricted diet suppressed physiological ^{18}F-FDG cardiac uptake completely (31). Therefore, following a protocol of prolonged fasting combined with appropriate dietary preparation is recommended to achieve complete suppression of physiological myocardial ^{18}F-FDG uptake.

On the basis of the above-mentioned reports, the Japanese Society of Nuclear Cardiology committee recommends the following pre-^{18}F-FDG PET/computed tomography (CT) fasting conditions.

Recommendations:
Fasting time for ^{18}F-FDG PET/CT in diagnosis of cardiac sarcoidosis

▶Prior to ^{18}F-FDG PET/CT, patients should fast for a minimum of 12 h, but up to 18 h if possible.
▶Since prolonged fasting preparation is sometimes insufficient to suppress physiological myocardial ^{18}F-FDG uptake, JSNC committee recommends following a carbohydrate-restricted diet in combination with prolonged fasting.

Precautions

It is essential to measure blood glucose levels before ^{18}F-FDG PET/CT studies. According to the ^{18}F-FDG PET/CT guidelines for oncological diagnosis or cardiac viability studies provided by the Society of Nuclear Medicine and Molecular Imaging (SNMMI) in the United States, ^{18}F-FDG PET/CT should be performed on the day after the blood glucose level is controlled if the fasting blood glucose level is 150–200 mg/dL (32). Given the above guidelines, the JSNC committee considers ^{18}F-FDG PET/CT to be unsuitable for patients with poorly controlled blood glucose levels.

Note: While an 18-h fast sounds quite long, it is achievable by scheduling an early afternoon PET study following overnight fasting after dinner at 6 p.m. on the day before the study. With such timing, 18 h fasting is feasible as a clinical practice.

2. Dietary modification prior to ^{18}F-FDG-PET/CT

Dietary modification makes it possible to have fatty acid metabolism exceed glucose metabolism and to suppress glucose metabolism in myocardium. Similar to changing the fasting time, following a specific diet may be effective in order to suppress myocardial physiological ^{18}F-FDG uptake (19, 25). A number of studies have looked at the effects of a low-carbohydrate diet alone or a low-carbohydrate/high-fat diet on suppressing physiological myocardial ^{18}F-FDG PET uptake

Table 2 Fasting time for ^{18}F-FDG PET and PET/CT

Author	Year	Pt (n)	Fasting time	Diet	Sensitivity (%)	Specificity (%)
Okumura et al. (67)	2004	22	>12 h	Not specified	100	91
Ishimaru et al. (47)	2005	32	>6 h	Not specified	100	82
Ohira et al. (48)	2008	21	>12 h	Not specified	88	39
Langah et al. (28)	2009	76	>18 h	Not specified	85	90
Tahara et al. (66)	2011	12	>12 h	Not specified	100	97
Yokoyama, et al. (37)	2015	92	>18 h	LCD	97	84
Momose, et al. (38)	2015	52	>12 h	LCD	100	72
Mean					95.7	79.3
Weighted Mean					94.6	81.2

LCD: low-carbohydrate diet
Reprinted with permission from (96).

Table 3 Diet preparation prior to ^{18}F-FDG PET/CT and myocardial ^{18}F-FDG uptake

Author	Year	Pt (n)	Materials	Fasting	Diet/Preparation	SUVmax
Williams et al. (36)	2008	161	malignancy	>4 h or overnight fasting		8.8 ± 5.7
				4 h	LCD+HFD	3.9 ± 3.6
Wykrzykowska et al. (40)	2009	32	suspected IHD	Overnight fast>8 h		8.8 ± 3.6
				no	LCD+HFD	2.5 ± 1.5
Cheng et al. (34)	2010	63	malignancy	>6 h	not specific	6.2 ± 5.2
				mean 15 h	LCD	3.3 ± 2.7
				mean 1 h	HFD	5.5 ± 4.2
Kobayashi et al. (35)	2013	14	normal volunteer	diet only	LCD+HFD	mean 1.31
Morooka et al. (29)	2014	37	normal volunteer	18 h		4.47 ± 4.31 (1.31–20.35)
				12 h	heparin	6.21 ± 3.64 (1.87–11.4)
Manabe et al. (30)	2017	190	malignancy	<12 h vs. >12 h	fasting only	5.5 ± 4.9 vs. 5.6 ± 4.6 (p=.0.92)
				<18 h vs. >18 h		5.9 ± 4.7 vs. 4.1 ± 4.0 (p=0.02)

HFD: high-fat diet, IHD: ischemic heart disease, LCD: low-carbohydrate diet, SUV: standardized uptake value
Reprinted with permission from (96).

(Table 3).

In an attempt to improve diagnostic accuracy in the assessment of intrathoracic cancer, Lum et al. recommended carbohydrate withdrawal the night before ^{18}F-FDG PET/CT. They showed significantly suppressed physiological ^{18}F-FDG uptake in the entire myocardium (33). Moreover, in a randomized study in patients with cancer, it was reported that following a low-carbohydrate diet resulted in significantly reduced ^{18}F-FDG uptake in the entire myocardium (34). Others reported that non-CS patients who followed a low-carbohydrate diet the day before ^{18}F-FDG-PET study had reduced physiological ^{18}F-FDG uptake in the heart [maximum standardized uptake value (SUVmax) 1.3–3.9)], which was significantly lower than the ^{18}F-FDG uptake found in ^{18}F-FDG PET studies performed under a prolonged fasting condition alone (34–36). The dietary protocol may also be applied to patients with CS. Recent studies have confirmed the suppression of physiological myocardial ^{18}F-FDG uptake in CS patients who followed these protocols (31, 37, 38). A low-carbohydrate diet is simple, clinically applicable, and recommended as a method of contributing to the accurate diagnosis of CS. In the low-carbohydrate diet, the carbohydrate content is less than 5 g per meal (34, 39, 40).

Ohira et al. provided a sample low-carbohydrate menu created by Hokkaido University Hospital (Figure 2A) (25). This sample menu includes a meal containing a boiled egg, tofu served in soy sauce topped with bonita flakes, and grilled chicken with carrots and cabbage. The nutritional breakdown of this sample menu is 4 g of carbohydrate, 20.6 g of protein and 5.6 g of fat (total 272 kcal) (Figure 2A). Another sample menu created by Ehime University Hospital includes a garden salad of red and green leaf lettuce topped with avocado cubes and a dressing of olive oil, soy sauce, vinegar, salt and pepper, and wakame seaweed soup. This menu includes a slice of low-

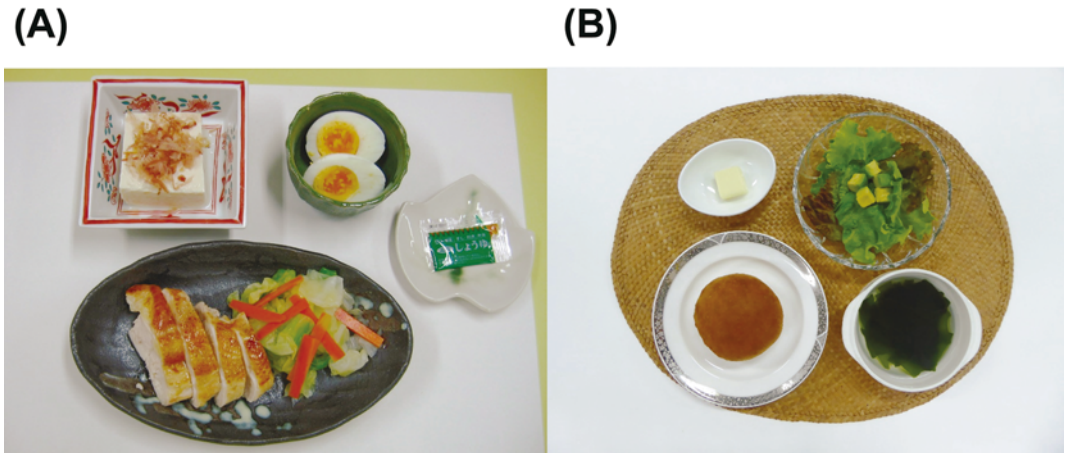

Fig. 2 Sample low-carbohydrate diet.
1. Sample recipe 1
This sample menu includes boiled egg, tofu in soy sauce topped with bonita flakes, and grilled chicken with carrots and cabbage. The nutrition of this sample menu includes 4 g of carbohydrate, 20.6 g of protein and 5.6 g of fat (total 272 kcal) (Figure 2A) (48).
2. Sample recipe 2
Another sample menu includes a garden salad with red and green leaf lettuce topped with avocado cubes covered in a dressing of olive oil, soy sauce, vinegar, salt and pepper, and wakame seaweed soup. This menu includes a slice of low-carbohydrate bread with butter (Figure 2B). The nutrition of this sample menu includes 4 g of carbohydrate, 9.5 g of protein and 16.4 g of fat (total 208 kcal) (Figure 2B)

Table 4 Sample foods for dietary preparation prior to ^{18}F-FDG PET/CT

Unsuitable food		Recommended	
beverages containing sugar	all sweet drinks e.g., juices alcoholic beverages, etc.	sugar-free drinking water	mineral water, tap water tea
food containing carbohydrates	starchy vegetables carrots tomatoes, etc. fruit all confections	low-carbohydrate vegetables	cabbage lettuce spinach Chinese cabbage broccoli green pepper cucumber
food with high carbohydrate content	cereals rice bread potato, sweet potato pumpkin corn, etc. noodles	low-carbohydrate food (protein and high-fat foods)	egg meat fish (note the seasoning)
			cheese butter (without sugar)
processed foods	fried chicken fried food, etc.		tofu (bean curd)
seasoning containing sugar (check ingredients and nutritional information)	processed sauces such as barbecue sauce	sugar-free seasoning	salt pepper soy sauce mayonnaise salad oil olive oil

carbohydrate bread with butter (Figure 2B). The nutritional breakdown of this sample menu is 4 g of carbohydrate, 9.5 g of protein and 16.4 g of fat (total 208 kcal) (Figure 2B). It is recommended that outpatients be given information regarding foods and drinks suitable for the diet protocol, as shown in Table 4.

It has also been shown that taking fatty acids suppresses myocardial glucose metabolism (41). Williams et al. at Beth Israel Deaconess Medical Center undertook a testing procedure in which they had patients follow a low-carbohydrate diet the

night before undergoing ^{18}F-FDG PET/CT and a high-fat diet 3 to 6 h before undergoing ^{18}F-FDG PET/CT. They reported that this method resulted in a significant reduction in ^{18}F-FDG uptake in the entire myocardium using SUVmax measurements (36, 40). Other researchers also reported that, in comparison with 12-h fasting alone, the above method resulted in significantly suppressed ^{18}F-FDG uptake in normal myocardium (42). In this case, the high-fat diet 4 h before administration of ^{18}F-FDG consisted of 20.8 g of fat and 1.2 g of carbohydrate (caloric intake of 265 kcal). Kobayashi et al. reported that 14 normal volunteers who followed the low-carbohydrate Atkins diet for 24 h and consumed a high-fat drink 1 hour before ^{18}F-FDG administration showed a complete lack of physiological cardiac ^{18}F-FDG uptake (35). However, it was not clarified whether the 24-h low-carbohydrate diet or the high-fat drink contributed more to reducing cardiac ^{18}F-FDG uptake in this study. No other articles demonstrated that a high-fat diet alone reduced cardiac physiological ^{18}F-FDG uptake. A consensus panel of the SNMMI recommends that patients eat a meal containing >35 g of fat as dietary preparation, but current JSNC guidelines consider that to be a supplementary pretreatment to a low-carbohydrate diet (19, 43).

Diabetic patients should have controlled blood glucose levels. Fasting for 18 hours or more can lead to hypoglycemia, and therefore a low-carbohydrate/high-fat diet is recommended. Reducing the hypoglycemic agent or insulin during preparation, in consultation with a diabetes physician, is recommended.

Recommendations:
Diet modification prior to ^{18}F-FDG PET/CT for the diagnosis of cardiac sarcoidosis

- Because 12 h to 18 h of fasting alone may result in variable myocardial ^{18}F-FDG uptake, it is also important to consider diet modification the night before undergoing ^{18}F-FDG PET/CT. It is recommended that patients have a low-carbohydrate meal the evening before undergoing ^{18}F-FDG PET/CT. In this case, the total carbohydrate content should be less than 5 g.
- Following a high-fat diet 3 to 6 h before administration of ^{18}F-FDG is also reportedly useful. However, the usefulness of this approach has yet to be established. This method will be the subject of future investigation.
- It is recommended that diabetic patients undergo the same ^{18}F-FDG PET/CT study as non-diabetic patients but with appropriate glycemic control.

Summary of Recommendations

In addition to a fasting time of 12 to 18 h, JSNC committee recommends changing the non-restricted diet before fasting to a low-carbohydrate diet. It is necessary to pay attention to hypoglycemia under prolonged fasting, especially in diabetic patients.

3. Pre-administration of unfractionated heparin

Intravenous administration of unfractionated heparin activates the serum lipoprotein lipase to increase free fatty acid (FFA) levels (44). Increased blood FFA levels suppress myocardial glucose metabolism and skeletal muscle glucose metabolism (45, 46). On the basis of these findings, a heparin pre-administration method was developed for ^{18}F-FDG PET in the diagnosis of CS (47). Blood FFA levels increase rapidly following heparin administration, and a protocol for intravenous administration of heparin 15 min before ^{18}F-FDG administration has been adopted (47). Nuutilla et al. (46) reported that the administered dose of heparin was 4,700 IU, although patients' body weights were unknown. Ishimaru et al. administered heparin at a dose of 50 IU/kg (47, 48). There has been no report examining the relationship between the dose of heparin and the suppression of myocardial ^{18}F-FDG uptake. According to a study by Asmal et al. (49) on the relationship between the dose of heparin and plasma FFA levels, a significant increase in FFA levels occurred after a bolus injection of 5 IU/kg of heparin. There was a further increase after 10 IU/kg, and a plateau was reached after a 15 IU/kg or greater dose of heparin.

Regarding the inhibitory effect of heparin pre-administration on myocardial ^{18}F-FDG uptake, a study by Ishimaru et al. of 30 healthy subjects with minimum 6-h fasting showed that myocardial ^{18}F-FDG uptake was not fully suppressed (14 cases, 47%), with the observation of diffuse myocardial ^{18}F-FDG uptake. Heparin pre-administration was considered to have the suppression effect only in some patients (47). Scholtens et al. compared ^{18}F-FDG PET scans of two groups, namely those who followed a low- carbohydrate diet (LCD) plus 12-h fasting and those who had an LCD plus 12-h fasting together with a 50 IU/kg heparin injection (50). Physiological myocardial ^{18}F-FDG uptake suppression was

significantly better in the group with heparin injection in addition to an LCD plus 12-h fasting, but inadequate cardiac suppression was still found in 12% of patients. Subsequently, Morooka et al. confirmed that for patients with known or suspected CS, an 18-h fast without an LCD was more effective for inhibiting physiological myocardial uptake than was a 12-h fast with heparin injection (29). They observed an inverse correlation between the SUVmax in the myocardium and baseline FFA levels before heparin injection, while no correlation was found between the SUVmax and insulin levels. Then, they suggested that physiological ^{18}F-FDG uptake was likely to be efficiently inhibited when the FFA level was more than 0.76 mEq/L. In a similar trial on the optimization of ^{18}F-FDG myocardial uptake suppression, Demeure et al. demonstrated by receiver-operating-characteristic analysis that an FFA level of more than 0.65 mEq/L had 68% sensitivity, 82% specificity, and 89% positive predictive value for predicting good ^{18}F-FDG uptake suppression. However, myocardial ^{18}F-FDG uptake suppression was not correlated with glucose or insulin level (51). Manabe et al. stated that an LCD with a minimum 18-h fast together with 50 IU/kg heparin pre-administration completely suppressed physiological ^{18}F-FDG uptake in 24 patients (31). On the other hand, 27.6% of patients with a minimum 6-h fast without LCD preparation showed diffuse myocardial uptake. The former group showed higher serum FFA than did the latter group before heparin administration. They also confirmed that patients with diffuse myocardial ^{18}F-FDG uptake had significantly lower FFA levels than did those without diffuse myocardial uptake *before* UFH injection. In this regard, low plasma FFA after the fasting preparation may be a predictive marker of diffuse physiological ^{18}F-FDG uptake, and higher FFA may predict successfully suppressive physiological ^{18}F-FDG uptake. Although serum FFA significantly increased in both groups 15 minutes after heparin administration, there was no significant difference in FFA levels between the two groups at that time. This finding may indicate that rapidly increasing FFA levels through the use of heparin does not have the effect of suppressing physiological myocardial ^{18}F-FDG uptake (52).

Based on those previous reports, low plasma FFA after the fasting preparation may be a predictive marker of diffuse physiological FDG uptake, and higher FFA may predict successfully suppressive physiological myocardial FDG uptake. Although the numbers of studies are limited, blood glucose level and plasma insulin level may not be predictive markers for physiological ^{18}F-FDG uptake.

Recommendation:
Pre-administration of unfractionated heparin

With a low-carbohydrate diet and a fast of more than 18 h, pre-injection of heparin may have a limited effect on the suppression of physiological myocardial ^{18}F-FDG uptake. Additionally, the risk of heparin-induced thrombocytopenia (HIT) should not be ignored. Therefore, administration of heparin before ^{18}F-FDG PET/CT is not recommended as a routine practice.

Precautions

Heparin administration is contraindicated in patients with a known bleeding tendency. Care must be taken to prevent the occurrence of heparin-induced thrombocytopenia (HIT). The incidence of HIT has been reported to vary from 0.5% to 5% (53) according to patient background, but a meta-analysis showed an HIT incidence of 2.6% (54). It is reported that previous exposure to heparin can lead to the formation of HIT antibodies. Patients can develop an HIT immune response at the second exposure to even a very small amount of heparin (55, 56). We do not yet have sufficient data to recommend an appropriate dose and regimen for heparin administration. Future studies comparing different doses and regimens are required.

[2] ^{18}F-FDG administration and ^{18}F-FDG PET scan protocol

1. ^{18}F-FDG administration dose

The ^{18}F-FDG PET, PET/CT Practice Guidelines 2012 of the Japanese Society of Nuclear Medicine (JSNM), published in September 2012, stipulate the methodology for ^{18}F-FDG PET/CT in the diagnosis of cardiac sarcoidosis (57). These guidelines recommend that an ^{18}F-FDG dose range from 111 MBq to 259 MBq (2 MBq/kg to 5 MBq/kg) for 3D data collection and from 185 MBq to 444 MBq (3 MBq/kg to 7 MBq/kg) for 2D data collection. The dose should be increased or decreased based on the type of PET/CT equipment to be used and the patient's age and body habitus.

ASNC imaging guidelines/SNMMI procedure standard for PET nuclear cardiology procedures (58) stipulate that the standard dose of ^{18}F-FDG in cardiac PET is in the 185 MBq–555 MBq (5 mCi–15 mCi) range for evaluation of

Table 5 Imaging protocols of the main studies on the application of ^{18}F-FDG PET in the diagnosis of cardiac sarcoidosis

Author	Year	Pt (n)	Equipment & mode[1)]	^{18}F-FDG dose	Interval for scan start	Cardiac spot imaging[2)]
Yamagishi et al. (68)	2003	17	PET (2D)	259–370 MBq	50 min	10 min
Okumura et al. (67)	2004	22	PET	200 MBq	60 min	Not specified
Ishimaru et al. (47)	2005	32	PET (3D)	185 MBq	45–60 min	Not specified
Langah et al. (28)	2009	20	PET/CT	555 MBq	60 min	Not specified
Tahara et al. (66)	2010	12	PET (3D)	4.2 MBq/kg	60 min	Not specified
Morooka et al. (29)	2014	202[#1]	PET/CT (3D)	370 MBq	60 min	10min/bed, Card. ⇒ WB (N.A. for 1 bed or 2beds)
Momose et al. (38)	2015	52	PET/CT (3D)	3.7 MBq/kg	60 min	20 min (10 min/bed × 2beds), WB ⇒ Card.
Manabe O et al. (31)	2016	82	PET (2D), PET/CT (3D)	3D PET/CT: 4.5 MBq/kg 2D PET: 185 MBq	60 min	WB only
Scholtens AM et al. (50)	2016	150[#2]	PET/CT (3D)	2 MBq/kg	60 min	Not specified
Ohira et al. (79)	2017	100	PET/CT (3D)	5 MB/kg	WB: 60 min Heart: 90 min	20 min (ECG-gated) WB ⇒ Card
Ishiyama M, et al. (93)	2017	16	PET/CT (2D & 3D)	259–407 MBq (7-11 mCi)	50–60 min	12 min/bed (2D), 8 min/bed (3D) Card. ⇒ WB, (N.A. for 1 bed or 2beds)

[1)] Equipment (mode): Acquisition mode is shown in parentheses. (Acquisition mode is not noted in this table if not available.)
[2)] Cardiac spot imaging: [Card. ⇒ WB] means that "cardiac spot imaging (Card.)" was first and "whole-body image (WB)" was obtained sequentially. [WB ⇒ Card.] means reverse order.
[#1] Of 202, 37 healthy subjects were included.
[#2] Of 150, 50 patients with malignant tumor were included.

myocardial viability, which is the same range recommended by the previous ASNC guideline PET Myocardial Perfusion and Glucose Metabolism Imaging (59). However, for the diagnosis of CS, these new guidelines have revised the dose of ^{18}F-FDG to be in the range of 296 MBq–370 MBq (8 mCi-10 mCi). With the same equipment, a lower dose is required for PET imaging for 3D data acquisition than for 2D data acquisition.

The main studies on the application of ^{18}F-FDG PET in the diagnosis of CS are listed in Table 5. All methods in these studies met the previous ASNC guidelines (59). Given the sensitivity of recent PET or PET/CT equipment and concerns about radiation exposure, a dose of 555 MBq is considered to be excessive (60, 61). In Japan, the dose recommended by the guidelines of the Japanese Society of Nuclear Medicine is thought to be more appropriate (57).

Recommendations:
^{18}F-FDG dose

- An intravenous dose in the range of 111 MBq to 259 MBq (2 MBq/kg to 5 MBq/kg) is recommended for 3D data acquisition. JSNC committee recommends a dose in the range of 185 MBq to 444 MBq (3 MBq/kg to 7 MBq/kg) for 2D data acquisition.
- The dose should be increased or decreased based on the type of PET or PET/CT equipment to be used and the patient's age and body habitus.

2. ^{18}F-FDG PET/CT scan protocol

The ^{18}F-FDG PET, PET/CT Practice Guidelines 2012 (57) of the JSNM stipulate the imaging method as follows: "Perform emission and transmission scanning (in PET) or CT scanning (in PET/CT) 45 to 60 min after ^{18}F-FDG administration with PET or PET/CT equipment."

Conversely, ASNC imaging guidelines/SNMMI procedure standard for PET nuclear cardiology procedures (58) recommend at least 45 min as an interval between ^{18}F-FDG administration and the start of the scan. However, ^{18}F-FDG uptake in the myocardium increases gradually with time even 45 min after ^{18}F-FDG administration, whereas uptake in the blood pool declines (62). Hence, for the diagnosis of CS, the ASNC/SNMMI guidelines recommend at least 60 min as the

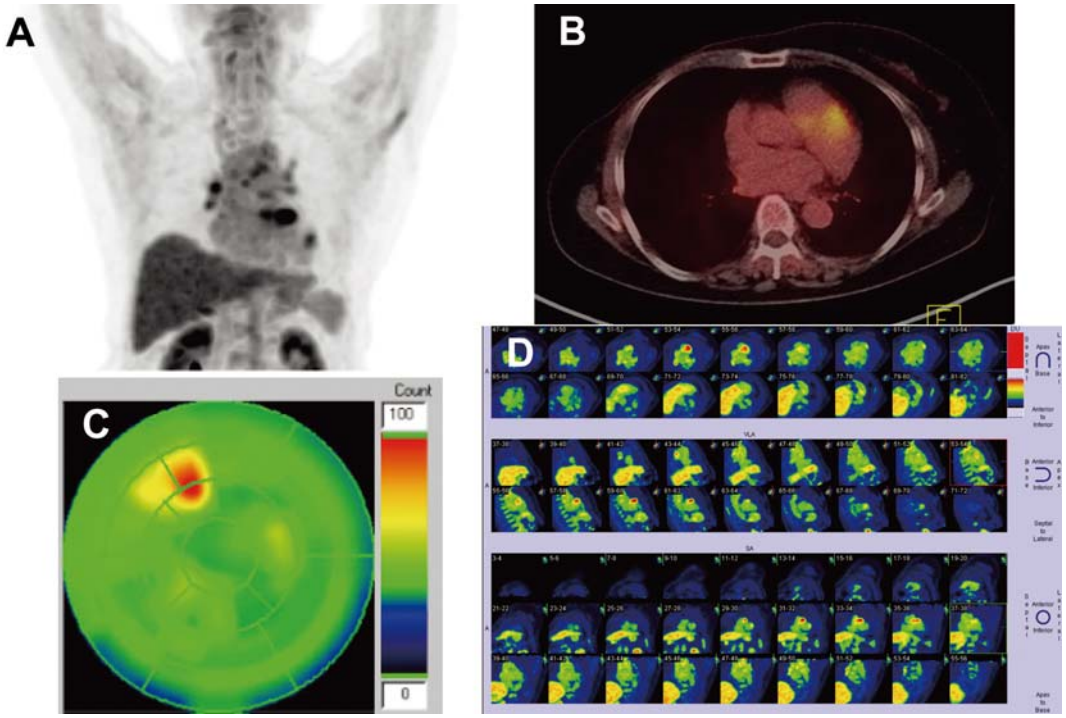

Figure 3 Display types of ^{18}F-FDG PET images for evaluating cardiac lesions.
In case of positive cardiac ^{18}F-FDG uptake with maximum intensity projection (MIP) image, additional image sets are recommended for detailed evaluation.
A: Systemic MIP image: MIP of thorax is indicated in this figure.
B: CT fusion image: trans-axial image is indicated in this figure.
C: Bull's eye map display.
D: Oblique tomography (upper: horizontal long axis/HL, middle: vertical long axis/ VL, lower: short axis/SA).
Reprinted with permission from (96).

interval between ^{18}F-FDG administration and the beginning of the scan, and ideally a 90-min interval if possible (19). However, the decrease in the radioactivity of ^{18}F-FDG due to the physical half-life of ^{18}F should also be taken into consideration. In this regard, in many previous studies, imaging was started 60 min after ^{18}F-FDG administration (Table 5) (Figure 1). It is important to standardize this time interval if ^{18}F-FDG PET and PET/CT imaging are performed repeatedly for follow-up.

Recommendations:
^{18}F-FDG PET or PET/CT imaging method

- Perform emission and transmission scanning (in conventional PET) or CT scanning (in PET/CT) 60 min to 90 min after ^{18}F-FDG administration.
- In subsequent imaging tests for comparison, the interval before the start of imaging (about 60 min) should be consistent with that applied for the previous imaging.

3. Spot cardiac imaging and avoidance of misalignment artifacts

When there is ^{18}F-FDG uptake in the heart with whole-body imaging, it is also recommended that cardiac spot imaging be performed after whole-body data acquisition (Figure 1). JMHLW approval for ^{18}F-FDG PET use is based on the detection of regions or disease activity of CS (16, 17), and spot cardiac imaging may provide more detailed information than might whole-body imaging (Figure 3).

According to ASNC imaging guidelines/SNMMI procedure standard for PET nuclear cardiology procedures (58), the data acquisition time is 10 min/1 bed in 3D data acquisition, and 20–30 min/1 bed in 2D data acquisition. A combination of respiratory gating and electrocardiographic gating is recommended if the PET/CT scanner allows for them. With the dose of ^{18}F-FDG based on the guidelines of the JSNM, a cardiac spot imaging time could be 10 min, which is considered to be sufficient. Issues for future studies could include the combined use of respiratory gating and electrocardiographic gating, optimal time of non-gated cardiac spot imaging, and

differences in SUV in the heart between spot images and whole-body images. Fig. 1 shows a typical acquisition protocol for ^{18}F-FDG PET imaging in the diagnosis of CS.

After imaging data acquisition, data are transferred to a dedicated workstation for image processing and analysis. In most previous studies on the use of PET in the diagnosis of CS, dedicated PET equipment was used. Up until now, PET/CT equipment has been used mainly in clinical settings. When using PET/CT equipment, it is important to avoid misregistration between the PET and CT images (see next section) (18). Misregistration generates image artifacts, which hinder comparison of the degrees of uptake among myocardial segments and the analysis of SUV (63). To prevent this misregistration, it is recommended that spot imaging of the heart with the patient's arms up be added to whole-body PET/CT scan imaging. Elevating the arms contributes to the reduction of streak artifacts or beam hardening in the heart. It is advisable to perform spot imaging of the heart by suppressing the movement of the diaphragm through abdominal compression or respiratory gating. If the patient has difficulty keeping their arms up, keeping arms in front of the body as much as possible is recommended. Doing so makes it possible to prevent the vertebral column and the arms, which are high X-ray absorbers, from being in the same straight line on the X-ray projection, and thus reduces streak artifacts or beam hardening.

Recommendations:
Cardiac spot imaging

- JSNC recommends performing cardiac spot imaging after whole-body data acquisition in the case of positive ^{18}F-FDG uptake with whole-body imaging. Spot imaging of the heart with the patient's arms elevated (duration of about 10 min) is recommended.
- In PET/CT imaging, it is important to avoid misregistration between the CT and PET images. The adoption of respiratory gating and electrocardiography gating may also be useful.

[3] ^{18}F-FDG PET image processing

1. Attenuation correction

PET scanners use transmission data for attenuation correction. Conventional PET scanner systems use radiation from an external source. On the other hand, PET/CT scanners use CT images for attenuation correction. However, since CT data are obtained in a shorter timeframe than are PET data, misregistration due to the patient's breathing and body movement can occur. Respiration-synchronization CT imaging (expiratory phase) makes it possible to avoid respiratory misalignment. However, availability of imaging equipment that has respiratory gating is currently limited. When misregistration between the PET and CT images is suspected, reference to original images without CT attenuation correction may be useful. The presence of a pacemaker lead, in particular an implantable cardioverter defibrillator (ICD) lead, may affect CT images. This metal artifact causes excessive attenuation correction and therefore care should be taken in interpreting images in such cases (64, 65).

2. Image reconstruction (short-axis, vertical long-axis, and horizontal long-axis)

Previous reports show that image reconstruction of myocardial tomography images was performed by oblique tomography (short-axis, vertical long-axis, and horizontal long-axis images) (27, 39, 47, 48, 66–68). However, if myocardial ^{18}F-FDG uptake is completely suppressed, it is difficult to perform such oblique tomography. In this case, axial chest tomography imaging (transverse, coronary, and sagittal tomographic imaging) is used (23). In oblique tomography, the central heart axis has to be set appropriately.

3. Bull's eye map display

It is useful to use a bull's eye map display on the basis of myocardial circumferential profile analysis of left ventricular (LV) short-axis images (display in polar coordinates) in confirming abnormal uptake distribution (Figure 3). This is also helpful for comparing images acquired using other modalities such as myocardial perfusion SPECT imaging with ^{18}F-FDG PET/CT images. Care should be taken in creating a bull's eye map display as follows:

(1) The myocardial trace should be performed accurately. If ^{18}F-FDG uptake is localized in the sarcoid lesion site, other normal myocardium does not have positive ^{18}F-FDG uptake. Thus, it may be difficult to trace myocardium.

(2) If the bull's eye map display is used for comparison with other images (SPECT MPI image, etc.), it is advisable to use the same workstation or algorithm to make the bull's eye map image since processing methods of apical and basal regions are different for each workstation and algorithm.

(3) Accuracy of the bull's eye map display should be confirmed through comparison with myocardial tomography.

Recommendations:
^{18}F-FDG PET/CT image processing and reconstruction

- When attenuation correction is conducted using CT images, attention should be paid to the potential occurrence of misregistration due to the patient's breathing or body motion. Comparison with original ^{18}F-FDG PET images without attenuation correction is useful. In patients with a pacemaker or an implanted ICD, care should be taken as a lead could affect CT images since metal induces artifacts and may cause excessive attenuation correction.
- If positive myocardial ^{18}F-FDG uptake is observed, oblique myocardial tomography imaging could be performed in addition to standard whole-body maximum intensity projection (MIP) imaging and axial chest tomography. If there is no myocardial uptake in the whole-body image, it is difficult to perform oblique myocardial tomography imaging.
- A bull's eye map display is useful for evaluating uptake location and patterns. It is also helpful for comparing ^{18}F-FDG images and other images including myocardial perfusion images. However, it is important to ensure that the bull's eye map display is appropriate by comparing it with myocardial tomography images. It is also important to use the same software and algorithm for comparison between the bull's eye map display and that from other modalities.

[4] ^{18}F-FDG PET image interpretation including diagnosis and risk analysis

The use of imaging data after attenuation correction is recommended. Overall assessment is conducted comprehensively, using whole-body MIP images, axial transverse tomography, LV short-axis image, LV vertical long-axis image, LV horizontal long-axis image, and bull's eye map display (Figure 3).

1. Whole-body ^{18}F-FDG PET MIP imaging for evaluation of systemic disease and axial transverse imaging

CS is considered to be a systemic disease including involvement of myocardium. Therefore, abnormal ^{18}F-FDG uptake in the lungs, lymph nodes, spleen, liver, muscles, eyes and skin should be observed using whole-body MIP images. However, there are some cases in which such abnormal ^{18}F-FDG uptake is not observed. The presence of isolated (no lesions except for the heart) CS has been reported (14, 69, 70). In some cases, visible cardiac involvement depends on the activity or stage of the disease. Abnormal ^{18}F-FDG uptake in the aortic wall (sarcoid vasculitis) can be observed on whole-body MIP images. Axial transverse images are helpful for observing the presence of abnormal ^{18}F-FDG uptake in the right ventricular free wall or atrial wall.

2. ^{18}F-FDG PET diagnostic criteria for cardiac lesions with visual assessment

Myocardial ^{18}F-FDG uptake distribution observed in CS has been visually analyzed on the basis of the classifications shown below:

1. Classification into three types of patterns (27): none, focal, and diffuse (Figure 4).

2. Classification into four types of patterns (47, 48, 66): none, focal, focal on diffuse, and diffuse.

Myocardial ^{18}F-FDG uptake distribution is classified into three types of patterns. According to the first classification, a focal pattern is considered to be a characteristic finding of abnormal ^{18}F-FDG uptake in a sarcoidosis inflammation lesion. The second classification, involving four types of patterns, was proposed by Ishimaru et al. (47). In that classification, a focal on diffuse pattern is considered to be a finding of localized abnormal ^{18}F-FDG uptake on a background of mild diffuse ^{18}F-FDG uptake, either due to physiological uptake or owing to heart failure as the heart metabolism shifts from fatty acid metabolism to glucose metabolism. In this regard, the focal on diffuse pattern could be included as part of the focal pattern. Figure 4 shows specific examples of these distribution patterns as described above. It has been reported that when patients with the focal and the focal on diffuse distribution patterns were determined to be positive for CS, by exclusion of cases with localized uptake only in the lateral wall, ^{18}F-FDG PET/CT imaging had a diagnostic capability of 100% and specificity of 81.5% (47).

In 2014, the Heart Rhythm Society issued a statement about a clinical diagnosis of cardiac sarcoidosis, which involved the presence of "patchy" myocardial ^{18}F-FDG uptake on dedicated cardiac PET together with a histological confirmation of extracardiac sarcoidosis (71). The JSNC committee is in agreement with the above statement and has hereby clarified the details regarding the "patchy" uptake.

3. Use of common sites of cardiac sarcoidosis as a reference

The base of the ventricular septum is known to be a common site of CS in association with wall thinning of the ventricular septum detected by echocardiography. Second- or third-degree atrioventricular block is observed in 23% to 30% of patients with CS, and it has been reported that this preponderance is related to inflammatory cell infiltration into the base of the ventricular septum (72, 73). Regional ^{18}F-FDG uptake was more frequent in patients with sarcoidosis with ECG abnormalities than in patients without ECG abnormali-

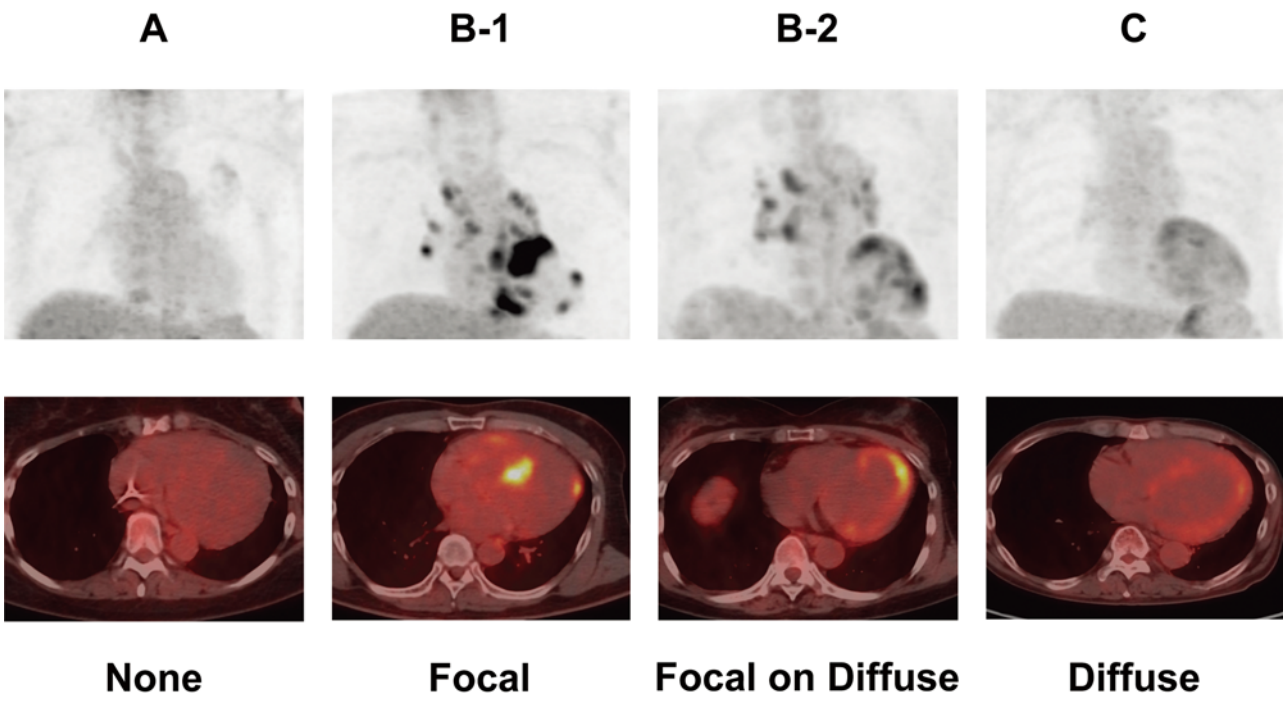

Figure 4 Diagnostic criteria for myocardial ^{18}F-FDG PET/CT imaging.

MIP images and transverse myocardial images.

A None: without focal myocardial ^{18}F-FDG uptake. This pattern is considered to be negative.

B-1 Focal: with localized ^{18}F-FDG uptake in the myocardium. This finding is considered to be positive for cardiac sarcoidosis. However, other heart diseases that show localized ^{18}F-FDG uptake (e.g. ischemic heart diseases and hypertrophic cardiomyopathy) must be excluded. ^{18}F-FDG uptake in the lateral wall region was reported even in healthy subjects (94, 95). Other researchers (47, 48) reported that localized ^{18}F-FDG uptake in this region does not indicate positivity for cardiac sarcoidosis. Other reports pointed out that localized ^{18}F-FDG uptake in the anteroseptal base and diffuse uptake in the entire circumference of the heart base could be physiological myocardial uptake (29, 79). Therefore, this remains a controversial issue. Care should be exercised in assessing the findings of ^{18}F-FDG uptake in these regions. Some researchers consider comparison of these false-positive findings with myocardial perfusion images to be useful for differential diagnosis.

B-2 Focal on diffuse: some strong ^{18}F-FDG uptake with diffuse myocardial uptake of ^{18}F-FDG. This finding generally indicates positivity for cardiac sarcoidosis. However, it requires careful interpretation because it has been reported that cases with such ^{18}F-FDG uptake potentially included false positive ones (55). In some patients with cardiac dysfunction and those with cardiac failure, diffuse myocardial ^{18}F-FDG uptake is sometimes observed under fasting conditions. Hence, the evaluation of findings is often difficult in these patients.

C Diffuse: definite diffuse ^{18}F-FDG uptake in the entire left ventricular wall without localized high ^{18}F-FDG uptake. This ^{18}F-FDG uptake distribution pattern generally does not indicate an abnormality, since it is histopathologically known that the myocardial sarcoidosis lesion is not diffuse but localized.

Reprinted with permission from (96).

ties. Among ECG abnormalities, AV block was associated with interventricular septum ^{18}F-FDG uptake (74). Localized ^{18}F-FDG uptake in the base of the ventricular septum in patients with atrioventricular block is likely to be at the active inflammatory lesion site and to be associated with clinical presentations. Based on these findings, looking at the location of ^{18}F-FDG uptake may be useful to distinguish between pathological uptake and physiological uptake.

On the other hand, a histopathological examination showed that the LV free wall is also a common site of CS (75). It was reported that ventricular tachycardia occurs in 23% of CS patients (72). If the onset site of monomorphic ventricular tachycardia corresponds to the ^{18}F-FDG positive uptake site, it is possible that it is the site of the lesion corresponding to the ventricular tachycardia.

4. ^{18}F-FDG uptake in the right ventricle

Non-caseating granuloma is seen in the right ventricle (RV) in 46% of cardiac sarcoidosis (76). Patients with RV involvement are at high risk of cardiac death and sustained ventricular tachycardia, and have appropriate indication for ICD cardioversion or antitachycardia pacing (77), although the mechanism of RV involvement with increased events is unknown.

With regard to the diagnostic value, patchy uptake of ^{18}F-FDG on the RV is a relatively specific finding for CS with high diagnostic accuracy (77). Echocardiography can reveal abnormal RV strain that is suspect for RV involvement in patients without pulmonary hypertension or lung diseases (78). Assessment of metabolic activity in the RV through ^{18}F-FDG PET is useful given its importance to patient management.

5. Quantitative analysis using standard uptake value (SUV)

SUV is determined by dividing uptake radioactivity post attenuation correction, as measured using a PET scanner, by radioactivity per kg of the patient's body weight. In CS, high SUV in the positive ^{18}F-FDG uptake site has been reported, consistent with visual assessment of the CS site (54). Okumura et al. divided the left ventricle into 13 segments. Patients with CS showed higher myocardial SUV than did healthy individuals. The diagnostic capability, on the basis of the above criterion, had a sensitivity of 100% and specificity of 91% (54). Tahara et al. divided the left ventricle into 17 segments and obtained SUV in each segment. The coefficient of variance of over 0.18 is regarded as positive for CS. This had a high diagnostic capability with sensitivity of 100% and specificity of 97% (55).

Furthermore, ^{18}F-FDG uptake was considered to be positive in several studies if its SUVmax in the left-ventricular myocardium was greater than the mean SUV in the right lobe of the liver (29, 74, 79, 80). Yokoyama et al. reported that the myocardial SUVmax with a cut-off value of 4.0 provided a sensitivity of 97.3% with a specificity of 83.6% for diagnosing CS under the strictest preparation methodology for ^{18}F-FDG PET (37). There are problems with the use of SUV in the diagnosis of CS that have yet to be solved. These include unstandardized SUV calculation software and differences in measurement values depending on imaging equipment and imaging conditions.

SUVmax captures a voxel with the highest intensity of ^{18}F-FDG uptake but does not delineate whether the ^{18}F-FDG uptake is focal or involves a large volume of myocardium. The extent of ^{18}F-FDG-positive lesions (e. g., SUV volume or volume of inflammation) can be measured by identifying voxels with an SUV intensity above a pre-defined threshold value (81). Ahmadian et al. proposed a new method to quantify the ^{18}F-FDG volume intensity, that is, cardiac metabolic volume (CMV; cm^3) and cardiac metabolic activity (CMA; g glucose) (82, 83). Further studies are needed to determine whether inclusion of these quantitative parameters will improve the diagnostic accuracy and prognostic value over a visual assessment of disease activity.

6. Prognostic marker of cardiac sarcoidosis

For the purpose of risk stratification in patients with CS, the following findings are useful to predict all-cause death, sustained ventricular tachycardia, and appropriated ICD cardioversion or anti-tachycardia pacing: These include 1) LV remodeling and function (84); 2) RV ^{18}F-FDG uptake (77); 3) ^{18}F-FDG uptake and perfusion defect in the same location. However, CS without these findings is also a risk factor in ventricular arrhythmia (85).

Whether the area and location of uptake, the SUVmax value, or the metabolic volume as shown through ^{18}F-FDG PET are associated with prognosis is unknown. In patients with suspected, but not definitive, CS, steroid therapy is often deferred, which results in poor outcomes compared to those for CS with steroid therapy (86). Accordingly, whether the use of steroid therapy should be guided by positive ^{18}F-FDG uptake needs to be evaluated.

7. Assessment of treatment response

^{18}F-FDG PET is reported to be useful for assessing the effects of immunosuppressive therapies (87). Serial ^{18}F-FDG PET studies should be performed with precisely the same preparation and data acquisition protocols, with the same dietary or fasting preparation, the same ^{18}F-FDG dose of administration, and the same interval between ^{18}F-FDG administration and image acquisition. Serial whole-body images may be helpful, since relying on cardiac images only may lead to normalization errors (88).

Yokoyama et al. compared ^{18}F-FDG PET/CT examinations before and after corticosteroid therapy quantitatively in 18 CS patents. Myocardial SUVmax significantly decreased in comparison with baseline values. Advanced atrioventricular block and/or frequent premature ventricular contractions disappeared in some patients, and brain natriuretic peptide (BNP) values significantly decreased after steroid therapy, while LV ejection fraction (EF) did not increase significantly (37). Osborne et al. examined 23 patients who had undergone a total of 90 serial PET examinations during treatment for cardiac sarcoidosis (83). In a longitudinal cohort, a reduction in the intensity and extent of myocardial inflammation area on ^{18}F-FDG PET was associated with improvement in LVEF. Ahmadian et al. also performed serial ^{18}F-FDG PET/CT studies (43 studies for 17 patients) before and after immunosuppression therapy (89). ^{18}F-FDG uptake was analyzed visually and quantitatively using SUVmax, CMV, and CMA with volume above SUV thresholds of 2.7 and 4.1 g/mL. Complete resolution of ^{18}F-FDG uptake was common using CMA and CMV, but a 2.7 g/mL SUV threshold and SUVmax were more likely to reveal partial responses. In 6 patients imaged after a dose reduction in immunosuppression, 4 had a rebound quantitative ^{18}F-FDG uptake.

Quantitative interpretation of ^{18}F-FDG PET/CT in CS can detect changes in ^{18}F-FDG uptake in response to immunosuppression. However, it should be acknowledged that a reduction in myocardial ^{18}F-FDG uptake has not been definitively proven to reflect the disease progression or natural history of CS. Larger, multi-center imaging studies in CS are needed to see if quantitative changes in ^{18}F-FDG uptake are associated with its outcomes.

Recommendations:
Image interpretation

- It is recommended that abnormal ^{18}F-FDG uptake in organs other than the heart be observed using whole-body MIP imaging and axial transverse imaging.
- ^{18}F-FDG uptake in the LV myocardium is classified into 3 patterns and a focal pattern is considered to be a characteristic finding of CS. A focal on diffuse pattern is considered to be a finding of localized abnormal uptake on a background of mild diffuse uptake either physiologically or in heart failure. Therefore, it would be included as part of the focal pattern. However, it is essential to exclude ischemic heart disease and hypertrophic cardiomyopathy. These diseases may trigger localized ^{18}F-FDG uptake.
- It is recommended that ^{18}F-FDG uptake in both RV and LV be evaluated since CS sometimes shows RV involvement.
- Since MPI, including SPECT and PET, is useful for confirming positive ^{18}F-FDG PET findings and disease staging in relation to the myocardial impairment site, the combined use of ^{18}F-FDG PET/CT and myocardial perfusion SPECT or PET is recommended in case of inconclusive ^{18}F-FDG PET findings.
- Measurement of SUV may be useful to improve diagnostic capability and quantify disease activity.

[5] ^{18}F-FDG PET image comparison with other imaging

1. Myocardial perfusion SPECT and PET

^{201}Tl- or ^{99m}Tc-labeled radiopharmaceutical SPECT and ^{13}N-ammonia or ^{82}Rubidium PET are useful in the evaluation of disease activity in CS. Although studies involving head-to-head comparison between pathological evaluation and myocardial perfusion abnormality are limited, perfusion defect reflects two types of injury of myocardium, namely reversible defect and irreversible scarring due to local inflammation. Steroid therapy is effective for reversible defect but not for scarring or LV aneurysm.

Four types of patterns in terms of ^{18}F-FDG PET findings (“none”, “diffuse”, “focal”, and “focal on diffuse”) are useful for diagnosing CS (18, 47). If ^{18}F-FDG uptake is consistent with the perfusion abnormality or is in the peripheral zone of the perfusion abnormality, there is likely to be a positive finding if coronary artery disease is excluded (77).

The diagnostic capability of myocardial perfusion SPECT is modest, with a sensitivity of 40% to 65% (50, 53). However, myocardial perfusion SPECT can be used to determine the stage of the disease for patients because it provides data on the state of myocardial tissue disorder: 1) Early stage: normal perfusion and positive ^{18}F-FDG uptake; 2) Advanced stage: perfusion defect and positive ^{18}F-FDG uptake; 3) End stage: perfusion defect and negative ^{18}F-FDG uptake (67).

Currently there is no available evidence of the usefulness of MPI alone without ^{18}F-FDG PET. Therefore the following areas need to be explored: 1) Screening and monitoring for cardiac involvement with MPI in patients with extracardiac sarcoidosis; 2) Screening for diagnosis of CS by using MPI in patients with advanced and complete atrioventricular block and ventricular arrhythmia; 3) Monitoring the effects of steroid therapy on myocardial perfusion. However, the evaluation of cardiac size and function with ECG-gated MPI can be useful in patients with CS.

The importance of MPI for CS diagnosis is also addressed in the previous guidelines and statement (12, 19, 71).

2. Myocardial fatty acid imaging

CS frequently involves a wider extent of defect of fatty acid analogue, as shown with ^{123}I-labelled β-methyl iodophenyl pentadecanoic acid (^{123}I-BMIPP), than does myocardial perfusion defect (38, 90). Momose et al. reported that the diagnostic ability of ^{123}I-BMIPP to differentiate CS from other heart failure was 74% in sensitivity and 80% in specificity, if perfusion and fatty acid metabolism mismatch defect score was >3 using both ^{123}I-BMIPP and ^{201}Tl on a 17-segment model (38). A ^{123}I-BMIPP defect region like perfusion defect is similar to high ^{18}F-FDG uptake lesions, but some CS patients in the early inflammation phase have neither ^{123}I-BMIPP nor ^{201}Tl defect. This finding indicates that a continued inflammatory process is required to develop myocardial damage or scarring. In addition, the mismatched area, with preserved perfusion but reduced ^{123}I-BMIPP uptake, showed quite a bit higher ^{18}F-FDG uptake. This may indicate that ^{123}I-BMIPP uptake was reduced prior to the development of perfusion defect in the active inflammatory region (91). There were few reports of ^{123}I-BMIPP use in CS patients because ^{123}I-BMIPP is approved for use only in Japan and is available only in a clinical setting (92). Further investigations are needed to establish the clinical roles of ^{123}I-BMIPP in CS patients.

Acknowledgments

The authors thank Ms. Kumiko Toshimitsu for providing a sample menu. This manuscript has been reviewed by a North American English-language professional editor, Ms. Holly Beanlands. The authors also thank Ms. Holly Beanlands for critical reading of the manuscript.

Sources of funding

None.

Conflicts of interest

None.

Reprint requests and correspondence:
Keiichiro Yoshinaga, MD, PhD, FACC, FASNC
Diagnostic and Therapeutic Nuclear Medicine, National Institutes for Quantum and Radiological Science and Technology, National Institute of Radiological Sciences, 4-9-1 Anagawa, Inage-Ku, Chiba, 263-8555, Japan
E−mail: yoshinaga.keiichiro@qst.go.jp

References

1. Iannuzzi MC, Rybicki BA, Teirstein AS. Sarcoidosis. N Engl J Med 2007; 357: 2153–65.
2. O'Regan A, Berman JS. Sarcoidosis. Ann Intern Med 2012; 156: ITC5-1, ITC5-2, ITC5-3, ITC5-4, ITC5-5, ITC5-6, ITC5-7, ITC5-8, ITC5-9, ITC5-10, ITC5-11, ITC5-12, ITC5-13, ITC5-14, ITC5-15; quiz ITC5-16.
3. Bargagli E, Prasse A. Sarcoidosis: a review for the internist. Intern Emerg Med 2018; 13: 325–31.
4. Silverman KJ, Hutchins GM, Bulkley BH. Cardiac sarcoid: a clinicopathologic study of 84 unselected patients with systemic sarcoidosis. Circulation 1978; 58: 1204–11.
5. Hiraga H HM, Iwai K. Guidelines for diagnosis of cardiac sarcoidosis: study report on diffuse pulmonary disease (in Japanese). Tokyo: The Japanese Ministry of Health and Welfare 1993: 2.
6. Diagnostic standard and guidelines for sarcoidosis. Jpn J Sarcoidosis and Granulomatous Disorders [in Japanese] 2007; 27: 89–102.
7. Iwai K, Sekiguti M, Hosoda Y, DeRemee RA, Tazelaar HD, Sharma OP, et al. Racial difference in cardiac sarcoidosis incidence observed at autopsy. Sarcoidosis 1994; 11: 26–31.
8. Ohira H, Yoshinaga K, Manabe O, Oyama-Manabe N, Tsujino I, Nishimura M, et al. Clinical application of ^{18}F-fluorodeoxyglucose PET and LGE CMR in cardiac sarcoidosis. Ann Nucl Cardiol 2017; 3: 125–30.
9. Patel AR, Kramer CM. Role of cardiac magnetic resonance in the diagnosis and prognosis of nonischemic cardiomyopathy. JACC Cardiovasc Imaging 2017; 10: 1180–93.
10. Uemura A, Morimoto S, Hiramitsu S, Kato Y, Ito T, Hishida H. Histologic diagnostic rate of cardiac sarcoidosis: evaluation of endomyocardial biopsies. Am Heart J 1999; 138: 299–302.
11. Cooper LT, Baughman KL, Feldman AM, Frustaci A, Jessup M, Kuhl U, et al. The role of endomyocardial biopsy in the management of cardiovascular disease: a scientific statement from the American Heart Association, the American College of Cardiology, and the European Society of Cardiology Endorsed by the Heart Failure Society of America and the Heart Failure Association of the European Society of Cardiology. Eur Heart J 2007; 28: 3076–93.
12. Terasaki F, Yoshinaga K. New guidelines for diagnosis of cardiac sarcoidosis in Japan. Ann Nucl Cardiol 2017; 3: 42–5.
13. Kandolin R, Lehtonen J, Airaksinen J, Vihinen T, Miettinen H, Ylitalo K, et al. Cardiac sarcoidosis: epidemiology, characteristics, and outcome over 25 years in a nationwide study. Circulation 2015; 131: 624–32.
14. Okada DR, Bravo PE, Vita T, Agarwal V, Osborne MT, Taqueti VR, et al. Isolated cardiac sarcoidosis: A focused review of an under-recognized entity. J Nucl Cardiol 2018; 25: 1136–46.
15. Nishiyama Y, Yamamoto Y, Fukunaga K, Takinami H, Iwado Y, Satoh K, et al. Comparative evaluation of ^{18}F-FDG PET and ^{67}Ga scintigraphy in patients with sarcoidosis. J Nucl Med 2006; 47: 1571–6.
16. Yoshinaga K, Maruno H, Chikamori T. Updated Japanese ministry of health, labour and welfare reimbursement policy for cardiac positron emission tomography and coronary intervention. Ann Nucl Cardiol 2018; 4: 42–5.
17. Yoshinaga K, Tamaki N. Current status of nuclear cardiology in Japan: Ongoing efforts to improve clinical standards and to establish evidence. J Nucl Cardiol 2015; 22: 690–9.
18. Ishida Y, Yoshinaga K, Miyagawa M, Moroi M, Kondoh C, Kiso K, et al. Recommendations for ^{18}F-fluorodeoxyglucose positron emission tomography imaging for cardiac sarcoidosis: Japanese Society of Nuclear Cardiology recommendations. Ann Nucl Med 2014; 28: 393–403.
19. Chareonthaitawee P, Beanlands RS, Chen W, Dorbala S, Miller EJ, Murthy VL, et al. Joint SNMMI-ASNC expert consensus document on the role of ^{18}F-FDG PET/CT in cardiac sarcoid detection and therapy monitoring. J Nucl Cardiol 2017; 24: 1741–58.
20. Yoshinaga K, Miyagawa M, Kiso K, Ishida Y. Japanese Guidelines for Cardiac Sarcoidosis. Ann Nucl Cardiol 2017; 3: 121–4.
21. Tamaki N, Manabe O, Yoshinaga K. Roles of ^{18}F-FDG PET in diagnosis and management of cardiac sarcoidosis − from the continuing medical education session at the 63rd SNMMI Meeting, June 2016. Ann Nucl Cardiol 2017; 3: 110–2.
22. Yoshinaga K, Tamaki N. Imaging myocardial metabolism. Curr Opin Biotechnol 2007; 18: 52–9.
23. Wisneski JA, Gertz EW, Neese RA, Mayr M. Myocardial metabolism of free fatty acids. Studies with ^{14}C-labeled substrates in humans. J Clin Invest 1987; 79: 359–66.
24. Miyagawa M, Tashiro R, Watanabe E, Kawaguchi N, Ishimura H, Kido T, et al. Optimal patient preparation for detection and assessment of cardiac sarcoidosis by FDG-PET. Ann Nucl Cardiol 2017; 3: 113–6.
25. Ohira H, Tsujino I, Yoshinaga K. ^{18}F-Fluoro-2-deoxyglucose positron emission tomography in cardiac sarcoidosis. Eur J Nucl Med Mol Imaging 2011; 38: 1773–83.
26. Boellaard R, O'Doherty MJ, Weber WA, Mottaghy FM, Lonsdale MN, Stroobants SG, et al. FDG PET and PET/CT: EANM procedure guidelines for tumour PET imaging: version 1.0. Eur J Nucl Med Mol Imaging 2010; 37: 181–200.
27. Youssef G, Leung E, Mylonas I, Nery P, Williams K, Wisenberg G, et al. The use of ^{18}F-FDG PET in the diagnosis of cardiac sarcoidosis: a systematic review and metaanalysis including the Ontario experience. J Nucl Med 2012; 53: 241–8.
28. Langah R, Spicer K, Gebregziabher M, Gordon L. Effectiveness of prolonged fasting ^{18}f-FDG PET-CT in the detection of

cardiac sarcoidosis. J Nucl Cardiol 2009; 16: 801–10.
29. Morooka M, Moroi M, Uno K, Ito K, Wu J, Nakagawa T, et al. Long fasting is effective in inhibiting physiological myocardial ^{18}F-FDG uptake and for evaluating active lesions of cardiac sarcoidosis. EJNMMI Res 2014; 4: 1.
30. Manabe O, Kroenke M, Aikawa T, Murayama A, Naya M, Masuda A, et al. Volume-based glucose metabolic analysis of FDG PET/CT: The optimum threshold and conditions to suppress physiological myocardial uptake. J Nucl Cardiol 2017. [Epub ahead of print]
31. Manabe O, Yoshinaga K, Ohira H, Masuda A, Sato T, Tsujino I, et al. The effects of 18-h fasting with low-carbohydrate diet preparation on suppressed physiological myocardial ^{18}F-fluorodeoxyglucose (FDG) uptake and possible minimal effects of unfractionated heparin use in patients with suspected cardiac involvement sarcoidosis. J Nucl Cardiol 2016; 23: 244–52.
32. Delbeke D, Coleman RE, Guiberteau MJ, Brown ML, Royal HD, Siegel BA, et al. Procedure Guideline for SPECT/CT Imaging 1.0. J Nucl Med 2006; 47: 1227–34.
33. Lum DP, Wandell S, Ko J, Coel MN. Reduction of myocardial 2-deoxy-2-[^{18}F] fluoro-D-glucose uptake artifacts in positron emission tomography using dietary carbohydrate restriction. Mol Imaging Biol 2002; 4: 232–7.
34. Cheng VY, Slomka PJ, Ahlen M, Thomson LE, Waxman AD, Berman DS. Impact of carbohydrate restriction with and without fatty acid loading on myocardial ^{18}F-FDG uptake during PET: A randomized controlled trial. J Nucl Cardiol 2010; 17: 286–91.
35. Kobayashi Y, Kumita S, Fukushima Y, Ishihara K, Suda M, Sakurai M. Significant suppression of myocardial ^{18}F-fluorodeoxyglucose uptake using 24-h carbohydrate restriction and a low-carbohydrate, high-fat diet. J Cardiol 2013; 62: 314–9.
36. Williams G, Kolodny GM. Suppression of myocardial ^{18}F-FDG uptake by preparing patients with a high-fat, low-carbohydrate diet. AJR Am J Roentgenol 2008; 190: W151–6.
37. Yokoyama R, Miyagawa M, Okayama H, Inoue T, Miki H, Ogimoto A, et al. Quantitative analysis of myocardial ^{18}F-fluorodeoxyglucose uptake by PET/CT for detection of cardiac sarcoidosis. Int J Cardiol 2015; 195: 180–7.
38. Momose M, Fukushima K, Kondo C, Serizawa N, Suzuki A, Abe K, et al. Diagnosis and detection of myocardial injury in active cardiac sarcoidosis－significance of myocardial fatty acid metabolism and myocardial perfusion mismatch. Circ J 2015; 79: 2669–76.
39. Ohira H, Tsujino I, Sato T, Yoshinaga K, Manabe O, Oyama N, et al. Early detection of cardiac sarcoid lesions with ^{18}F-fluoro-2-deoxyglucose positron emission tomography. Intern Med 2011; 50: 1207–9.
40. Wykrzykowska J, Lehman S, Williams G, Parker JA, Palmer MR, Varkey S, et al. Imaging of inflamed and vulnerable plaque in coronary arteries with ^{18}F-FDG PET/CT in patients with suppression of myocardial uptake using a low-carbohydrate, high-fat preparation. J Nucl Med 2009; 50: 563–8.
41. Frayn KN. The glucose-fatty acid cycle: a physiological perspective. Biochem Soc Trans 2003; 31: 1115–9.
42. Harisankar CN, Mittal BR, Agrawal KL, Abrar ML, Bhattacharya A. Utility of high fat and low carbohydrate diet in suppressing myocardial FDG uptake. J Nucl Cardiol 2011; 18: 926–36.
43. Bois JP, Chareonthaitawee P. Patient page-sarcoidosis imaging. J Nucl Cardiol 2017. [Epub ahead of print]
44. Persson E. Lipoprotein lipase, hepatic lipase and plasma lipolytic activity. Effects of heparin and a low molecular weight heparin fragment (Fragmin). Acta Med Scand Suppl 1988; 724: 1–56.
45. Shulman GI, Rothman DL, Jue T, Stein P, DeFronzo RA, Shulman RG. Quantitation of muscle glycogen synthesis in normal subjects and subjects with non-insulin-dependent diabetes by ^{13}C nuclear magnetic resonance spectroscopy. N Engl J Med 1990; 322: 223–8.
46. Nuutila P, Koivisto VA, Knuuti J, Ruotsalainen U, Teräs M, Haaparanta M, et al. Glucose-free fatty acid cycle operates in human heart and skeletal muscle *in vivo*. J Clin Invest 1992; 89: 1767–74.
47. Ishimaru S, Tsujino I, Takei T, Tsukamoto E, Sakaue S, Kamigaki M, et al. Focal uptake on ^{18}F-fluoro-2-deoxyglucose positron emission tomography images indicates cardiac involvement of sarcoidosis. Eur Heart J 2005; 26: 1538–43.
48. Ohira H, Tsujino I, Ishimaru S, Oyama N, Takei T, Tsukamoto E, et al. Myocardial imaging with ^{18}F-fluoro-2-deoxyglucose positron emission tomography and magnetic resonance imaging in sarcoidosis. Eur J Nucl Med Mol Imaging 2008; 35: 933–41.
49. Asmal AC, Leary WP, Thandroyen F, Botha J, Wattrus S. A dose-response study of the anticoagulant and lipolytic activities of heparin in normal subjects. Br J Clin Pharmacol 1979; 7: 531–3.
50. Scholtens AM, Verberne HJ, Budde RP, Lam MG. Additional heparin preadministration improves cardiac glucose metabolism suppression over low-carbohydrate diet alone in ^{18}F-FDG PET imaging. J Nucl Med 2016; 57: 568–73.
51. Demeure F, Hanin FX, Bol A, Vincent MF, Pouleur AC, Gerber B, et al. A randomized trial on the optimization of ^{18}F-FDG myocardial uptake suppression: implications for vulnerable coronary plaque imaging. J Nucl Med 2014; 55: 1629–35.
52. Bois JP, Chareonthaitawee P. Optimizing radionuclide imaging in the assessment of cardiac sarcoidosis. J Nucl Cardiol 2016; 23: 253–5.
53. Jang IK, Hursting MJ. When heparins promote thrombosis: review of heparin-induced thrombocytopenia. Circulation 2005; 111: 2671–83.
54. Martel N, Lee J, Wells PS. Risk for heparin-induced thrombocytopenia with unfractionated and low-molecular-weight heparin thromboprophylaxis: a meta-analysis. Blood 2005; 106: 2710–5.
55. Muslimani AA, Ricaurte B, Daw HA. Immune heparin-induced thrombocytopenia resulting from preceding exposure to heparin catheter flushes. Am J Hematol 2007; 82: 652–5.
56. Kato S, Takahashi K, Ayabe K, Samad R, Fukaya E, Friedmann P, et al. Heparin-induced thrombocytopenia: analysis of risk factors in medical inpatients. Br J Haematol 2011; 154: 373–7.
57. FDG PET, PET/CT Practice guidelines 2012, September 2012 by Japanese Society of Nuclear Medicine. Kaku Igaku 2012; 49: 391–401.
58. Dilsizian V, Bacharach SL, Beanlands RS, Bergmann SR,

Delbeke D, Dorbala S, et al. ASNC imaging guidelines/SNMMI procedure standard for positron emission tomography (PET) nuclear cardiology procedures. J Nucl Cardiol 2016; 23: 1187–226.
59. Machac J, Bacharach SL, Bateman TM, Bax JJ, Beanlands R, Bengel F, et al. Positron emission tomography myocardial perfusion and glucose metabolism imaging. J Nucl Cardiol 2006; 13: e121–51.
60. Cerqueira MD, Allman KC, Ficaro EP, Hansen CL, Nichols KJ, Thompson RC, et al. Recommendations for reducing radiation exposure in myocardial perfusion imaging. J Nucl Cardiol 2010; 17: 709–18.
61. Kudo T. Present status of medical radiation and nuclear cardiology usage in Japan: a discussion at the American Society of Nuclear Cardiology joint symposium. Ann Nucl Cardiol 2018; 4: 142–8.
62. Hays MT, Segall GM. A mathematical model for the distribution of fluorodeoxyglucose in humans. J Nucl Med 1999; 40: 1358–66.
63. Schwaiger M, Ziegler S, Nekolla SG. PET/CT: challenge for nuclear cardiology. J Nucl Med 2005; 46: 1664–78.
64. DiFilippo FP, Brunken RC. Do implanted pacemaker leads and ICD leads cause metal-related artifact in cardiac PET/CT? J Nucl Med 2005; 46: 436–43.
65. Ghafarian P, Aghamiri SM, Ay MR, Rahmim A, Schindler TH, Ratib O, et al. Is metal artefact reduction mandatory in cardiac PET/CT imaging in the presence of pacemaker and implantable cardioverter defibrillator leads? Eur J Nucl Med Mol Imaging 2011; 38: 252–62.
66. Tahara N, Tahara A, Nitta Y, Kodama N, Mizoguchi M, Kaida H, et al. Heterogeneous myocardial FDG uptake and the disease activity in cardiac sarcoidosis. JACC Cardiovasc Imaging 2010; 3: 1219–28.
67. Okumura W, Iwasaki T, Toyama T, Iso T, Arai M, Oriuchi N, et al. Usefulness of fasting ^{18}F-FDG PET in identification of cardiac sarcoidosis. J Nucl Med 2004; 45: 1989–98.
68. Yamagishi H, Shirai N, Takagi M, Yoshiyama M, Akioka K, Takeuchi K, et al. Identification of cardiac sarcoidosis with ^{13}N-NH_3/^{18}F-FDG PET. J Nucl Med 2003; 44: 1030–6.
69. Tavora F, Cresswell N, Li L, Ripple M, Solomon C, Burke A. Comparison of necropsy findings in patients with sarcoidosis dying suddenly from cardiac sarcoidosis versus dying suddenly from other causes. Am J Cardiol 2009; 104: 571–7.
70. Kandolin R, Lehtonen J, Salmenkivi K, Räisänen-Sokolowski A, Lommi J, Kupari M. Diagnosis, treatment, and outcome of giant-cell myocarditis in the era of combined immunosuppression. Circ Heart Fail 2013; 6: 15–22.
71. Birnie DH, Sauer WH, Bogun F, Cooper JM, Culver DA, Duvernoy CS, et al. HRS expert consensus statement on the diagnosis and management of arrhythmias associated with cardiac sarcoidosis. Heart Rhythm 2014; 11: 1305–23.
72. Banba K, Kusano KF, Nakamura K, Morita H, Ogawa A, Ohtsuka F, et al. Relationship between arrhythmogenesis and disease activity in cardiac sarcoidosis. Heart Rhythm 2007; 4: 1292–9.
73. Kandolin R, Lehtonen J, Kupari M. Cardiac sarcoidosis and giant cell myocarditis as causes of atrioventricular block in young and middle-aged adults. Circ Arrhythm Electrophysiol 2011; 4: 303–9.
74. Manabe O, Ohira H, Yoshinaga K, Sato K, Klaipetch A, Oyama-Manabe N, et al. Elevated ^{18}F-fluorodeoxyglucose uptake in the interventricular septum is associated with atrioventricular block in patients with suspected cardiac involvement sarcoidosis. Eur J Nucl Med Mol Imaging 2013; 40: 1558–66.
75. Roberts WC, McAllister HA Jr, Ferrans VJ. Sarcoidosis of the heart. A clinicopathologic study of 35 necropsy patients (group 1) and review of 78 previously described necropsy patients (group 11). Am J Med 1977; 63: 86–108.
76. Nelson JE, Kirschner PA, Teirstein AS. Sarcoidosis presenting as heart disease. Sarcoidosis Vasc Diffuse Lung Dis 1996; 13: 178–82.
77. Blankstein R, Osborne M, Naya M, Waller A, Kim CK, Murthy VL, et al. Cardiac positron emission tomography enhances prognostic assessments of patients with suspected cardiac sarcoidosis. J Am Coll Cardiol 2014; 63: 329–36.
78. Patel MB, Mor-Avi V, Murtagh G, Bonham CA, Laffin LJ, Hogarth DK, et al. Right heart involvement in patients with sarcoidosis. Echocardiography 2016; 33: 734–41.
79. Ohira H, Ardle BM, deKemp RA, Nery P, Juneau D, Renaud JM, et al. Inter- and intraobserver agreement of ^{18}F-FDG PET/CT image interpretation in patients referred for assessment of cardiac sarcoidosis. J Nucl Med 2017; 58: 1324–9.
80. Paquet N, Albert A, Foidart J, Hustinx R. Within-patient variability of ^{18}F-FDG: standardized uptake values in normal tissues. J Nucl Med 2004; 45: 784–8.
81. Manabe O, Ohira H, Yoshinaga K, Naya M, Oyama-Manabe N, Tamaki N. Qualitative and quantitative assessments of cardiac sarcoidosis using ^{18}F-FDG PET. Ann Nucl Cardiol 2017; 3: 117–20.
82. Ahmadian A, Brogan A, Berman J, Sverdlov AL, Mercier G, Mazzini M, et al. Quantitative interpretation of FDG PET/CT with myocardial perfusion imaging increases diagnostic information in the evaluation of cardiac sarcoidosis. J Nucl Cardiol 2014; 21: 925–39.
83. Osborne MT, Hulten EA, Singh A, Waller AH, Bittencourt MS, Stewart GC, et al. Reduction in ^{18}F-fluorodeoxyglucose uptake on serial cardiac positron emission tomography is associated with improved left ventricular ejection fraction in patients with cardiac sarcoidosis. J Nucl Cardiol 2014; 21: 166–74.
84. Chiu CZ, Nakatani S, Zhang G, Tachibana T, Ohmori F, Yamagishi M, et al. Prevention of left ventricular remodeling by long-term corticosteroid therapy in patients with cardiac sarcoidosis. Am J Cardiol 2005; 95: 143–6.
85. Betensky BP, Tschabrunn CM, Zado ES, Goldberg LR, Marchlinski FE, Garcia FC, et al. Long-term follow-up of patients with cardiac sarcoidosis and implantable cardioverter-defibrillators. Heart Rhythm 2012; 9: 884–91.
86. Takaya Y, Kusano KF, Nakamura K, Ito H. Comparison of outcomes in patients with probable versus definite cardiac sarcoidosis. Am J Cardiol 2015; 115: 1293–7.
87. Birnie DH, Nery PB, Beanlands RS. Clinical management of cardiac sarcoidosis. Ann Nucl Cardiol 2017; 3: 131–6.
88. Waller AH, Blankstein R. Quantifying myocardial inflammation using F18-fluorodeoxyglucose positron emission tomography in cardiac sarcoidosis. J Nucl Cardiol 2014; 21: 940–3.

89. Ahmadian A, Pawar S, Govender P, Berman J, Ruberg FL, Miller EJ. The response of FDG uptake to immunosuppressive treatment on FDG PET/CT imaging for cardiac sarcoidosis. J Nucl Cardiol 2017; 24: 413–24.
90. Kaminaga T, Takeshita T, Yamauchi T, Kawamura H, Yasuda M. The role of iodine-123-labeled 15-(p-iodophenyl)-3R, S-methylpentadecanoic acid scintigraphy in the detection of local myocardial involvement of sarcoidosis. Int J Cardiol 2004; 94: 99–103.
91. Kataoka S, Momose M, Fukushima K, Serizawa N, Suzuki A, Kondo C, et al. Regional myocardial damage and active inflammation in patients with cardiac sarcoidosis detected by non-invasive multi-modal imaging. Ann Nucl Med 2017; 31: 135–43.
92. Manabe O, Kikuchi T, Scholte AJHA, El Mahdiui M, Nishii R, Zhang MR, et al. Radiopharmaceutical tracers for cardiac imaging. J Nucl Cardiol 2018; 25: 1204–36.
93. Ishiyama M, Soine LA, Vesselle HJ. Semi-quantitative metabolic values on FDG PET/CT including extracardiac sites of disease as a predictor of treatment course in patients with cardiac sarcoidosis. EJNMMI Res 2017; 7: 67.
94. Bartlett ML, Bacharach SL, Voipio-Pulkki LM, Dilsizian V. Artifactual inhomogeneities in myocardial PET and SPECT scans in normal subjects. J Nucl Med 1995; 36: 188–95.
95. Gropler RJ, Siegel BA, Lee KJ, Moerlein SM, Perry DJ, Bergmann SR, et al. Nonuniformity in myocardial accumulation of fluorine-18-fluorodeoxyglucose in normal fasted humans. J Nucl Med 1990; 31: 1749–56.
96. Kumita S, Yoshinaga K, Miyagawa M, Momose, M, Kiso K, Kasai T, et al. Recommendation for ^{18}F-FDG PET Imaging for cardiac sarcoidosis. Shinzo-Kaku-Igaku 21: 22-27_14.https://doi.org/10.14951/jsnc.21-001